



Deposited via The University of Sheffield.

White Rose Research Online URL for this paper:

<https://eprints.whiterose.ac.uk/id/eprint/212058/>

Version: Accepted Version

Book Section:

Li, Y. and Qin, N. (2022) Load control on the future greener aircraft by circulation control. In: Knoerzer, D., Periaux, J. and Tuovinen, T., (eds.) *Advances in Computational Methods and Technologies in Aeronautics and Industry. Computational Methods in Applied Sciences*, 57. Springer International Publishing, pp. 105-116. ISBN: 9783031120183. ISSN: 1871-3033. EISSN: 2543-0203.

https://doi.org/10.1007/978-3-031-12019-0_8

This version of the book chapter has been accepted for publication, after peer review (when applicable) and is subject to Springer Nature's AM terms of use, but is not the Version of Record and does not reflect post-acceptance improvements, or any corrections. The Version of Record is available online at: http://dx.doi.org/10.1007/978-3-031-12019-0_8

Reuse

Items deposited in White Rose Research Online are protected by copyright, with all rights reserved unless indicated otherwise. They may be downloaded and/or printed for private study, or other acts as permitted by national copyright laws. The publisher or other rights holders may allow further reproduction and re-use of the full text version. This is indicated by the licence information on the White Rose Research Online record for the item.

Takedown

If you consider content in White Rose Research Online to be in breach of UK law, please notify us by emailing eprints@whiterose.ac.uk including the URL of the record and the reason for the withdrawal request.

Load Control on the Future Greener Aircraft by Circulation Control

Yonghong Li^{1,2}, Ning Qin^{1,}*

1.University of Sheffield, Sheffield, England S1 3JD, United Kingdom

2.China Aerodynamics Research and Development Center, Mianyang 621000, China

Load control is an important topic in aerodynamics, as it can potentially provide an alternative way for drag reduction through decreasing the aircraft structure weight. To pursue ‘Green Aviation’, both new greener aircraft configurations and technologies for load control are under studying throughout the worldwide industries and academies. This paper presents a computational investigation on the load control effects by means of circulation control (CC) via blowing over trailing-edge Coanda surface on a blended-wing-body (BWB) configuration. A BWB model is firstly modified to include Coanda devices on the outer-wing, inner-wing and center-body sections with the same spanwise length. The load control effects in terms of lift reduction aiming for gust load alleviation of CC placed on different spanwise locations are evaluated and compared under steady conditions for subsonic and transonic speeds. The results show that CC has a strong capability for load control, especially for subsonic incoming flow, indicating a promising way for gust load alleviation to replace the traditional flaps.

Nomenclature

C_L	=	lift coefficient
C_D	=	drag coefficient
C_{mx}	=	root bending moment coefficient
L/D	=	lift-to-drag ratio
C_μ	=	momentum coefficient

* Professor of Aerodynamics, Department of Mechanical Engineering, Corresponding Author, n.qin@sheffield.ac.uk.

U_∞ = freestream velocity
 M = Mach number
 α = angle of attack
 C_p = pressure coefficient
 c_{ref} = mean aerodynamic chord length
 Re = Reynolds number
 x, y, z = Cartesian coordinates in streamwise, spanwise and vertical directions
 η = the span length ratio

1. Introduction

In EUROPE's vision for future air transport, Fight Path 2050 [1], published by the Advisory Council for Aeronautics Research in Europe in 2011, sets a challenging target for a 75% reduction of CO₂ emissions from 2000 reference, which necessitates significant further reduction of aerodynamic drag for future aircraft. To achieve these objectives, a series of technologies and various novel aircraft concept designs have been investigating for future aircraft design with a better aerodynamic performance. BWB configurations, also known as the hybrid-wing body (HWB), have been studied for past few decades. Some results including the geometric design parameters and aerodynamic characteristics are available in the literature. BWB research models includes the Boeing first and second-generation BWB models [2] for the BWB design study, the BWB model for the EU MOB project [3], SAX-40 model [4] investigated by Cambridge and MIT for the feasibility of low noise and fuel efficiency, as well as the N2-A/B/EXTE HWB designs [5, 6] by Boeing to meet the ERA program's N+2 targets. These configurations have been served as the basis for various kinds of studies. Typically, based on the second-generation of Boeing-BWB design, Lyu *et al*, [7] built a similar planform shape for aerodynamic design optimization studies. To simplify the model, the nacelle and the winglet are not included. The authors [8] investigated the influence of spanwise load distributions on the overall performance on a similar planform of the 2nd-generation of Boeing-BWB design, *etc.* These studies provide useful insights into the aerodynamic performance of the BWB designs.

For technologies aiming for drag reduction, such as shock control [9-12], laminar flow control [13-19], turbulent drag reduction [20-23], etc., have been studied for decades. However, the lack of application of these technologies mentioned above on current aircraft indicates that there are still great challenges in science, especially in terms of

practical application. Recently, more focuses have been given to the study on load control, as it provides an alternative way for drag reduction through decreasing the weight of the aircraft structure. It is well known that the mass of the structure is not determined by the cruise condition but is dictated by the critical load cases such as gust and maneuvering loads. Guo *et al.* [24] indicated that the gust load can be greater than the maneuvering load and produces the most critical load cases in structure design for some aircraft. To ensure aircraft safety, Airworthiness authorities have specified typical gust models associated with parameters as requirement for aircraft certification. To cope with these critical load cases, the aircraft structure has to be robust, strong and resilient enough to withstand the forces and stress induced by gusts with a large amount of mass penalty because it is challenging to design an aircraft structure which is both light and robust. However, from another point of view, if the load on the aircraft can be controlled timely to deal with the gusts, a lighter structure may be designed without compromising safety.

Fluidic actuators, such as steady blowing or suction, synthetic jets and oscillating jets, have been investigated as means of active aerodynamic flow control methods for many years. But most of these studies focused on altering the momentum balance of the boundary layer to achieve aerodynamic improvement. For example, on top of transition delay and drag reduction, these methods have been proven to be effective to prevent flow separation and augment lift. A wide range of active flow control studies can be found on the subjects of flow mechanism [25, 26], comparison of effectiveness of different actuators [27, 28], parameter studies including geometry parameters [29], injection or suction parameters [30-32] and excitation parameters [33], influence of locations and layouts [34]. Some significant breakthroughs have been achieved using fluidic actuators for improving aerodynamic performance. Instead of lift augmentation, fluidic actuators can also be used in reducing and managing lift, to find alternative ways for gust load alleviation.

More recently, flapless control using circulation control (CC) by Coanda effect has attracted much attention. CC using Coanda effect to alter the circulation around the aircraft wings to generate additional forces for flight control attracted much attention in the recent years. The Coanda effect describes the tendency of a fluidic jet to stay attached to a convex surface as a result of a balance between the low static pressures generated by the jet and the centrifugal force acting on the curving jet. The jet entrains the external flow to follow the jet as to “bend down” over the curved surface which produces a net increase in the circulation of the wing resulting in lift augmentation. Similarly, lift reduction can be achieved if the jet slot is placed on the lower surface. Alexander *et al.* [35] conducted a number of experiments to test the effectiveness of CC for lift augmentation or reduction under steady conditions. Numerical work

has been done to validate the numerical methods for the simulation of CC by Min *et al.* [36] and Forster and Steijl [37]. The results show that RANS with $k-\omega$ SST turbulence model is able to capture the changes of pressure distributions on the airfoil caused by CC. The design and optimization of Coanda surface and the effectiveness of CC as means of maneuverability control of fixed and rotary-wing aircraft have also been studied numerically by Forster and Steijl [37] and Cook et al. [38]. Based on the 2-D NACA 0012 airfoil, a numerical investigation on the gust load alleviation effects by CC from subsonic to transonic speeds had been carried out in our previous study in [39].

As can be seen, initial researches have been carried out for the test of CC as a maneuver effector to replace conventional control surfaces. But no attention has been given to evaluate the capability of CC for load control on the future greener aircraft. In this paper, the lift reduction effects aiming for gust load alleviation on a BWB model were studied from subsonic to transonic speed.

2. BWB Model with Trailing-Edge Coanda Devices

Based on the 2nd-generation of Boeing-BWB design, the authors have set up a similar planform shape for the investigation of spanwise load distributions on the overall performance in [8]. The geometry was created from the lofting of an airfoil profile stack to conform to the prescribed planform shape. The modified NASA SC(2)-0414 airfoil with a reduced maximum camber from 1.5% to 0.5%, NASA SC(2)-0412 and SC(2)-0410 were used at the center plane, mid-span section and the wing tip, respectively. In this study, the same BWB geometry as shown in Fig. 1 is used here. The colour on the right differentiates the wing and the center body of the BWB.

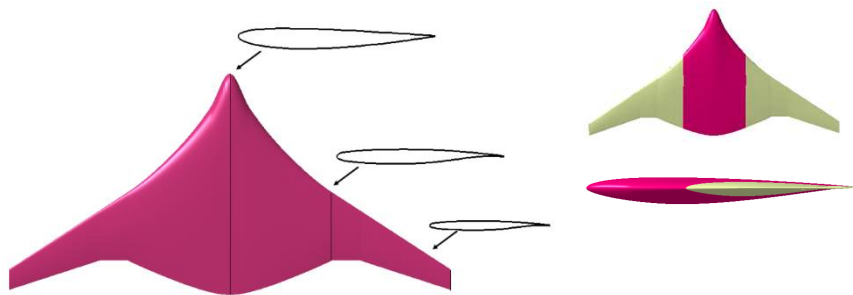


Fig. 1 The BWB model

In order to include the trailing-edge Coanda device on the SACCON model, G. Hoholis [40] truncated the existing wings at the required thickness and created a new semi-circular trailing edge. As the supercritical aerofoils used widely in the modern commercial aircraft wings tend to have a low thickness ratio, especially at the rear region, modification by truncating the trailing edge will reduce many areas of the wing resulting in a significant decrease of

the lift at the same angle of attack as the baseline model. On the numerical study of CC of a supercritical aerofoil, M. Forster [41] modified the airfoil by increasing the thickness of the trailing edge along the camber line, which was proved to have a little influence on the aerodynamic characteristics. Here, a similar modification was applied to the baseline BWB model. The rear 30% of the wing airfoil was thickened symmetrically around the camber line. The geometry parameter of the Coanda surface used for the BWB model is the same as it used in the previous 2-D airfoil study in [39]. To be specific, the trailing-edge Coanda surface has a semi-circular trailing edge with a radius of 0.5% of the local chord length, and the height of the slot exit is 1:20 to the radius. Based on the radius of the trailing edge, the increment of the thickness of the airfoil trailing edge on each section along the spanwise direction can be calculated for the Coanda surface design. Fig. 2 shows the comparison of the airfoil sections between the baseline and the modified one at the spanwise section of $\eta=0.5$ respectively.

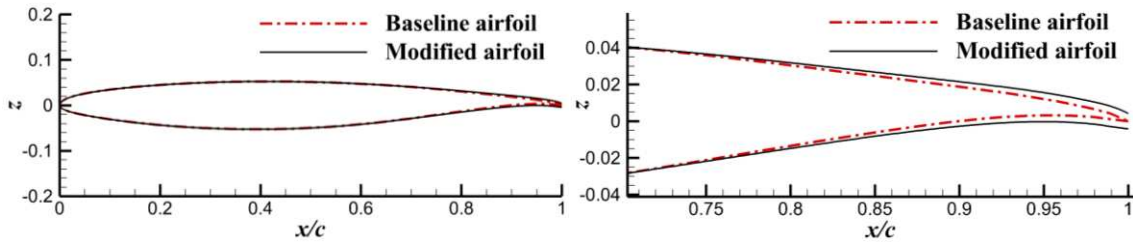


Fig. 2 Comparison of the airfoil section between the baseline and the modified one

In order to test the efficiency of CC deployed on different spanwise locations, three slots with equal spanwise length as shown in Fig. 3 on the center body, inner wing, and outer wing, respectively, are studied.

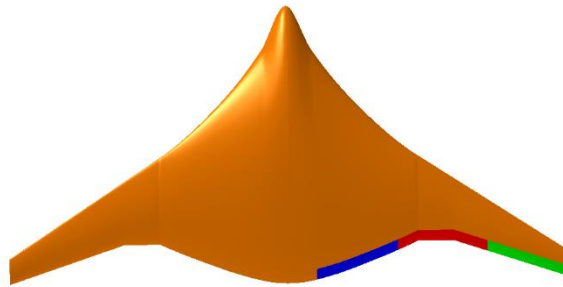


Fig. 3 The locations of CC on the BWB model

A. Grid Convergence

The NASA open CFD software CFL3D [42] is used for this work. The validation of CFL3D for the simulation of CC has been presented in [39] based on the experimental data conducted by Alexander *et al.* [35]. Identical to the

boundary settings in the validation study, the varying of the momentum coefficient (C_μ) is through adjusting the nozzle pressure ration (NPR; $p_{t,i}/p_\infty$); this is the pressure ratio between the air in the plenum chamber and the freestream flow. k- ω SST turbulence model is used for the study.

Based on the knowledge of the grid requirement through the grid convergence study in the CC validation in [39], a baseline grid has been generated on the BWB model as shown in Fig. 4. The number of the total cells of the baseline grid is about 7×10^6 in the half span domain. From this, a coarser and a finer grid were generated with a refinement factor of about 1.5 in each direction. Table 1 gives the effects of grid resolutions on the lift, drag and root bending moment coefficients at $M=0.8$, $\alpha=2.5^\circ$, $Re=5.2 \times 10^6/m$ under a blowing momentum coefficient $C_\mu=1.78 \times 10^{-4}$. A Richardson extrapolation was performed to estimate the aerodynamic coefficients with an ‘infinite’ grid by $C_{cont} = C_{23.6m} + (C_{23.6m} - C_{7.0m})/(r^2 - 1)$, where $r=1.5$. As shown in the results, for the lift coefficient, the grid with 7×10^6 cells produced result that was within 1.7% of the continuum estimate, and it was less than 3% for the drag and root bending moment coefficients. From these results, it was indicated that the medium grid gave reasonably accurate results while with computational cost efficiency.

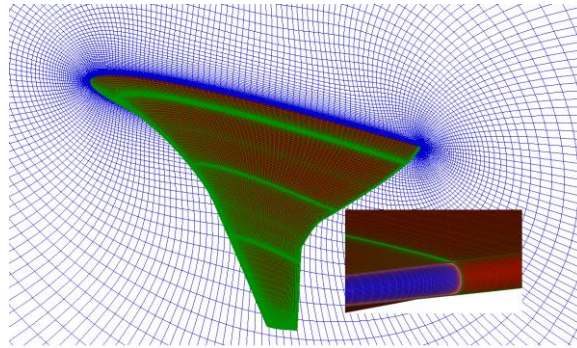


Fig. 4 Grid detail on the trailing edge near the center body

Table 1 Effects of grid resolutions on aerodynamic coefficients at $M=0.8$, $\alpha=2.5^\circ$, $C_\mu=1.78 \times 10^{-4}$

Grid size	2.1×10^6	7.0×10^6	23.6×10^6	Continuum
C_L	0.1307	0.1315	0.1328	0.1338
C_D	0.01085	0.01073	0.01064	0.01056
C_{mx}	0.0602	0.0611	0.0621	0.0629

B. Evaluation of the Influence of the Coanda Device on the BWB Performance

To understand how the modifications made to the BWB model influences the aerodynamic behaviour, the aerodynamic coefficients are compared between the models before and after the modification over a range of angles

of attack under $M=0.8$ as shown in Fig. 5. The results indicate that the influence of the thickened trailing edge and CC device is small, especially on the lift coefficient. The CC device produces slightly more drag at the lower angles of attack with an approximate 0.0004 penalty in the drag coefficient. This drag penalty results in approximately 3.8% reduction in the lift to drag ratio under the cruise condition ($C_L=0.23$). The influence on drag coefficients declines with increasing angles of attack.

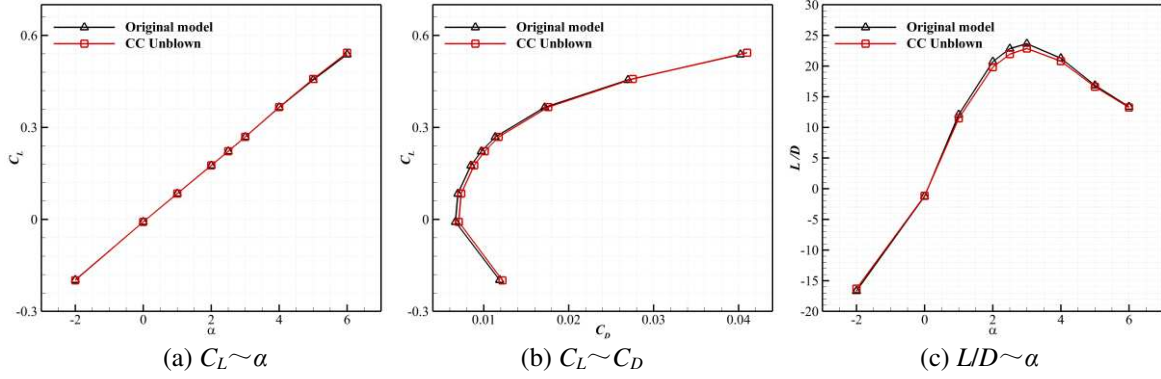


Fig. 5 Comparison of the aerodynamic performance between unblown CC model and the initial shape

3. Load Control Performance of CC

To get an understanding of the load control performance of CC deployed on the three different locations, the load control effects in terms of lift and root bending moment at a range of momentum coefficients are compared under subsonic and transonic steady conditions.

A. Transonic Case at $M=0.8$

Fig. 6 presents the comparisons of load control effects in terms of lift coefficient reduction at cruise condition. As expected, the outer wing located CC has the lowest maximum lift reduction compared to another two located CC, which is due to the smaller chord length and wing area. The maximum ability of outer-wing CC in terms of lift coefficient reduction is only -0.016, while it is -0.041 and -0.063 for the models with CC on the inner wing and center body, respectively. Also shown in Fig. 6 is that the ' C_{μ} -stall' occurs at a similar NPR value of around 2.4 for these three located CC. Therefore, the utmost ability of these three located CC for lift coefficient reduction and root bending moment reduction can be evaluated as shown in Table 2. As can be seen that the center body CC generates the most lift coefficient reduction of -0.063 which is four times of the capability from the outer-wing CC, but the maximum

root bending moment reduction by these two CC is similar. The inner-wing CC has a stronger capability for root bending moment relief as a maximum value of -0.015 can be obtained.

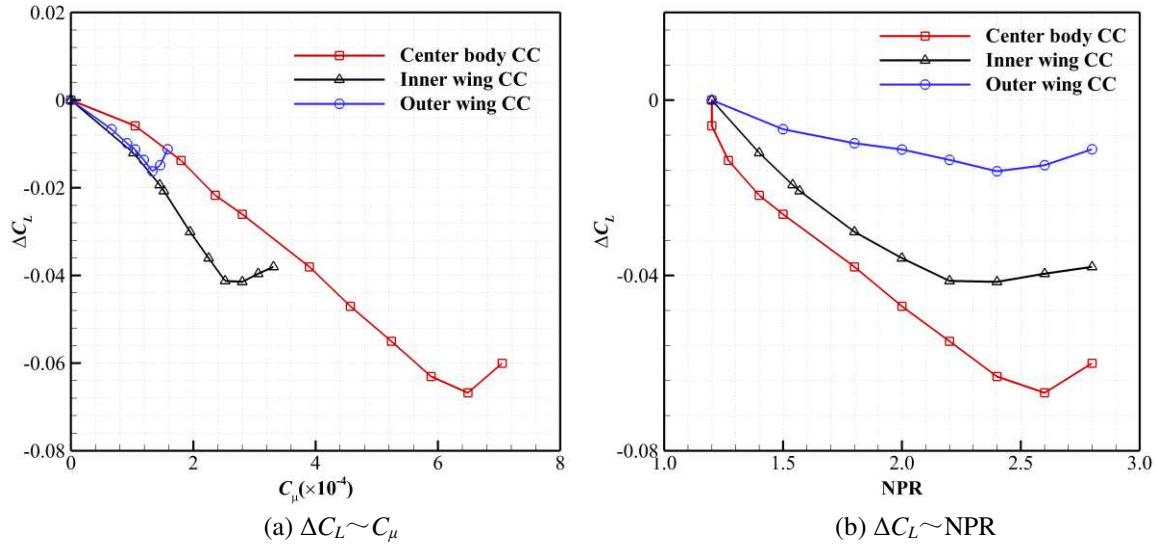


Fig. 6 Comparison of lift reduction for different location of CC

Table 2 The utmost ability of CC for lift coefficient and root bending moment coefficient reduction

Model	C_L	ΔC_L	C_{mx}	ΔC_{mx}
Unblown	0.222	---	0.0779	---
Center body CC	0.159	-0.063	0.0684	-0.0095
Inner wing CC	0.181	-0.041	0.0627	-0.0152
Outer wing CC	0.205	-0.016	0.0678	-0.0101

It has been demonstrated from the 2-D case studies in [39] that at transonic speed, the CC capability is reduced compared to subsonic range. Therefore, for the 3-D BWB model, if the CC is only deployed on finite spanwise location, the load control capability will be further reduced. It is expected that the three-located CC should work together to obtain a significant load control effect. The efficiency of the three-located CC working together is tested under NPR= 2.4. The total reduction in root bending moment and lift coefficients is given in Table 3. The maximum reduction of -0.125 in lift coefficient and -0.036 in root bending moment coefficient is obtained. The comparisons of the spanwise local lift coefficients between the three-located CC working together and the unblown model are given in Fig. 7. Significant reduction in local lift coefficients along the entire span has been obtained.

Table 3 Three located CC working together for lift and root bending moment coefficients reduction

Model	C_L	ΔC_L	C_{mx}	ΔC_{mx}
Unblown	0.222	---	0.0779	---
CC working together	0.097	-0.125	0.0419	-0.036

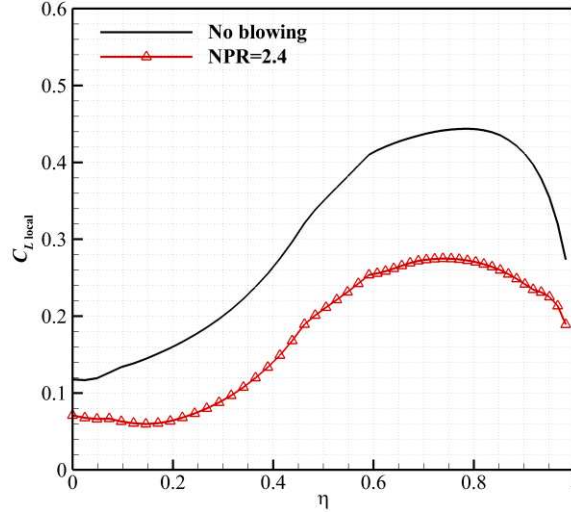


Fig. 7 The influence on spanwise local lift coefficient of the three located CC working together

B. Subsonic Case at $M=0.3$

For subsonic range, the lift reduction effects by the three located CC working together are tested at $M=0.3$, $Re=6.98 \times 10^6$ /m. The results are compared with the data at $M=0.8$, as shown in Fig. 8. For $M=0.3$, the simulation is conducted under $C_L=0.403$ corresponding to the angle of attack of 6° for the estimation to support the same aircraft weight as that under the cruise condition.

As can be seen from the results that CC has a much stronger control ability at $M=0.3$ than $M=0.8$, which is the same as the results demonstrated previously on the 2-D airfoil in [39]. The maximum lift coefficient reduction is up to -0.44 at $M=0.3$ compared to the value of only -0.125 at $M=0.8$. Fig. 9 shows the comparisons of spanwise local lift coefficients between CC model with $C_{\mu}=1.28 \times 10^{-3}$ and the baseline model at $M=0.3$. The spanwise local lift coefficients decrease significantly under CC. For instance, at $\eta=0.6$, the local lift coefficient for the baseline model is 0.68, while this value is only 0.36 for the CC model with $C_{\mu}=1.28 \times 10^{-3}$.

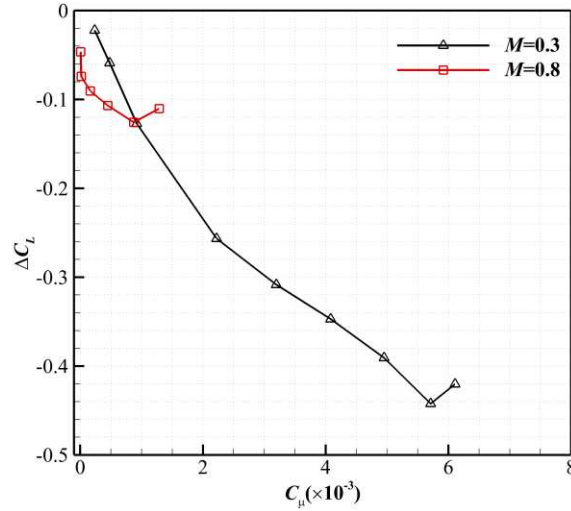


Fig. 8 Comparison of lift reduction between $M=0.3$ and $M=0.8$

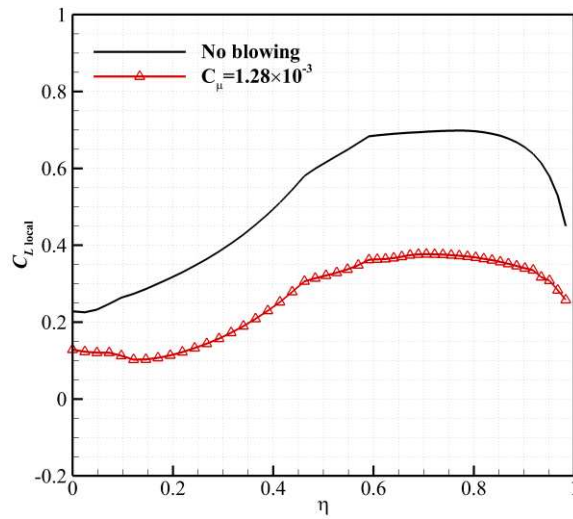


Fig. 9 Comparison of local spanwise lift coefficient at $M=0.3$

4. Conclusion

Load control effects by circulation control via blowing over trailing-edge Coanda surface have been tested on a BWB model. The BWB model is firstly modified to include the Coanda devices on the trailing edges and the influence of the modification on the aerodynamic performance is assessed relative to the baseline model. Load control effects of CC placed on different spanwise locations are evaluated and compared under steady conditions at $M=0.3$ and 0.8 . The results indicate that the thickened trailing edge to install CC devices has little influence on the aerodynamic performance, especially for the lift coefficient. The CC devices introduce an approximate 4 more drag counts penalty at the cruise condition relative to the baseline model. For the designed CC located from center body to outer wing

working together, the utmost load control capability in terms of lift coefficient reduction under steady conditions is up to -0.44 and -0.125 for $M= 0.3$ and 0.8 , respectively. Significant spanwise load reduction along the whole span by CC is obtained, indicating its promising load control capability. Compared to CC located on the center body and outer wing, CC can achieve higher load control effects on the inner wing sections.

References

1. Salam, I.R. and C. Bil, *Multi-disciplinary analysis and optimisation methodology for conceptual design of a box-wing aircraft*. Aeronaut. J., 2016. **120**(1230): p. 1315-1333.
2. Liebeck, R.H., *Design of the Blended Wing Body Subsonic Transport*. Journal of Aircraft, 2004. **41**(1): p. 10-25.
3. Qin, N., et al., *Aerodynamic considerations of blended wing body aircraft*. Progress in Aerospace Sciences, 2004. **40**(6): p. 321-343.
4. Hileman, J.I., et al., *Airframe Design for Silent Fuel-Efficient Aircraft*. Journal of Aircraft, 2010. **47**(3): p. 956-969.
5. Gatlin, G., D. Vicroy, and M. Carter, *Experimental Investigation of the Low-Speed Aerodynamic Characteristics of a 5.8-Percent Scale Hybrid Wing Body Configuration*, in *30th AIAA Applied Aerodynamics Conference*. Paper 2012-2669, 2012.
6. Bahr, C.J., et al. *Acoustic Data Processing and Transient Signal Analysis for the Hybrid Wing Body 14- by 22-Foot Subsonic Wind Tunnel Test*. in *20th AIAA/CEAS Aeroacoustics Conference*. Paper 2014-2345, 2014.
7. Lyu, Z. and J.R.R.A. Martins, *Aerodynamic Design Optimization Studies of a Blended-Wing-Body Aircraft*. Journal of Aircraft, 2014. **51**(5): p. 1604-1617.
8. Li, Y. and N. Qin, *Influence of Spanwise Load Distribution on Blended-Wing-Body Performance at Transonic Speed*. Journal of Aircraft, 2020. **0**(0): p. 1-10.
9. Colliss, S.P., et al., *Vortical structures on three-dimensional shock control bumps*. Journal of Aircraft, 2016. **53**(4): p. 2338-2350.
10. K. Bruce, P.J. and H. Babinsky, *Experimental Study into the Flow Physics of Three-Dimensional Shock Control Bumps*. Journal of Aircraft, 2012. **49**(5): p. 1222-1233.
11. König, B., et al., *Numerical and Experimental Validation of Three-Dimensional Shock Control Bumps*. Journal of Aircraft, 2009. **46**(2): p. 675-682.
12. Ogawa, H., et al., *Shock-Wave/Boundary-Layer Interaction Control Using Three-Dimensional Bumps for Transonic Wings*. AIAA Journal, 2008. **46**(6): p. 1442-1452.
13. Messing, R. and M.J. Kloker, *Investigation of suction for laminar flow control of three-dimensional boundary layers*. J. Fluid Mech., 2010. **658**: p. 117-147.
14. Chernoray, V.G., et al., *Experiments on secondary instability of streamwise vortices in a swept-wing boundary layer*. J. Fluid Mech., 2005. **534**: p. 295-325.
15. Krishnan, K.S.G., O. Bertram, and O. Seibel, *Review of hybrid laminar flow control systems*. Progress in Aerospace Sciences, 2017. **93**: p. 24-52.
16. Brion V, Dandois J, Mayer R, Reijasse P, Lutz T, Jacquin L. Laminar buffet and flow control. Proceedings of the Institution of Mechanical Engineers, Part G: Journal of Aerospace Engineering. 2020;234(1):124-139. doi:10.1177/0954410018824516
17. Ashill, P.R., J.L. Fulker, and K.C. Hackett, *A review of recent developments in flow control*. Aeronautical Journal, 2005. **109**(1095): p. 205-232.
18. Joslin, R.D., *Overview of Laminar Flow Control - NASA/TP-1998-208705*. 1998, Sponsoring Organization: NASA Langley Research Center.
19. *Boeing Commercial Aircraft Company, Hybrid laminar flow control study final report*, NASA-CR-165930. 1982.
20. Murai, Y., *Frictional drag reduction by bubble injection*. Experiments in Fluids, 2014. **55**(7): p. 1-28.
21. Fuaad, P.A., M.F. Baig, and B.A. Khan, *Turbulent drag reduction using active control of buoyancy forces*. International Journal of Heat and Fluid Flow, 2016. **61**: p. 585-598.
22. Ahmad, H., M.F. Baig, and P.A. Fuaad, *Numerical investigation of turbulent-drag reduction induced by active control of streamwise travelling waves of wall-normal velocity*. European Journal of Mechanics / B Fluids, 2015. **49**: p. 250-263.
23. Wang, Y.-S., W.-X. Huang, and C.-X. Xu, *Active control for drag reduction in turbulent channel flow: the opposition control schemes revisited*. Fluid Dynamics Research, 2016. **48**(5): p. 055501.
24. Guo, S., J. Los, and Y. Liu, *Gust Alleviation of a Large Aircraft with a Passive Twist Wingtip*. Aerospace, 2015. **2**(2): p. 135-154.
25. Hu, J., R. Wang, and D. Huang, *Flow control mechanisms of a combined approach using blade slot and vortex generator in compressor cascade*. Aerospace Science and Technology, 2018. **78**: p. 320-331.
26. Itsariyapinyo, P. and R.N. Sharma, *Large Eddy simulation of a NACA0015 circulation control airfoil using synthetic jets*.

- Aerospace Science and Technology, 2018. **82-83**: p. 545-556.
27. Shmilovich, A. and Y. Yadlin, *Flow Control Techniques for Transport Aircraft*. AIAA Journal, 2011. **49**(3): p. 489-502.
 28. Hammerton, J.R., et al., *Optimum distributed wing shaping and control loads for highly flexible aircraft*. Aerospace Science and Technology, 2018. **79**: p. 255-265.
 29. Yousefi, K., R. Saleh, and P. Zahedi, *Numerical study of blowing and suction slot geometry optimization on NACA 0012 airfoil*. Journal of Mechanical Science and Technology, 2014. **28**(4): p. 1297-1310.
 30. Luedke, J., et al., *Characterization of Steady Blowing for Flow Control in a Hump Diffuser*. AIAA Journal, 2005. **43**(8): p. 1644-1652.
 31. Chen, C., R. Seele, and I. Wagnanski, *Flow Control on a Thick Airfoil Using Suction Compared to Blowing*. AIAA Journal, 2013. **51**(6): p. 1462-1472.
 32. Zhang, H., et al., *Flow separation control using unsteady pulsed suction through endwall bleeding holes in a highly loaded compressor cascade*. Aerospace Science and Technology, 2018. **72**: p. 455-464.
 33. Greenblatt, D. and I.J. Wagnanski, *The control of flow separation by periodic excitation*. Progress in Aerospace Sciences, 2000. **36**(7): p. 487-545.
 34. Gebhardt, A. and J. Kirz, *Numerical investigation of slot variations on the efficiency of tangential blowing at a vertical tailplane with infinite span*. An Official Journal of the Council of European Aerospace Societies, 2018. **9**(1): p. 195-206.
 35. Alexander, M.G., et al., *Trailing Edge Blowing on a Two-Dimensional Six-Percent Thick Elliptical Circulation Control Airfoil Up to Transonic Conditions - NASA/TM-2005-213545*. 2005, Sponsoring Organization: NASA Langley Research Center.
 36. Min, B.-Y., et al., *Numerical Investigation of Circulation Control Airfoils*. Journal of Aircraft, 2009. **46**(4): p. 1403-1410.
 37. Forster, M. and R. Steijl, *Design study of Coanda devices for transonic circulation control*. The Aeronautical Journal, 2017. **121**(1243): p. 1368-1391.
 38. Cook, M.V., A. Buonanno, and S.D. Erbslöh, *A circulation control actuator for flapless flight control*. The Aeronautical Journal, 2016. **112**(1134): p. 483-489.
 39. Li, Y. and N. Qin, *Airfoil gust load alleviation by circulation control*. Aerospace Science and Technology, 2020. **98**: p. 105622.
 40. Hoholis, G., R. Steijl, and K. Badcock, *Circulation Control as a Roll Effector for Unmanned Combat Aerial Vehicles*. Journal of Aircraft, 2016. **53**(6): p. 1875-1889.
 41. Forster, M. and R. Steijl, *Numerical Simulation of Transonic Circulation Control*. 53rd AIAA Aerospace Sciences Meeting, AIAA 2015-1709, 2015.
 42. Krist, S.L., C.L. Rumsey, and R.T. Biedron, *CFL3D User's Manual (Version 5.0) - NASA/TM-1998-208444*. 1998, Sponsoring Organization: NASA Langley Research Center.